Antitumor Agents

DOI: 10.1002/ange.201409161

Direct Cytosolic Delivery of siRNA Using Nanoparticle-Stabilized Nanocapsules**

*Ying Jiang, Rui Tang, Bradley Duncan, Ziwen Jiang, Bo Yan, Rubul Mout, and Vincent M. Rotello**

Abstract: *The use of nanoparticle-stabilized nanocapsules (NPSCs) for the direct cytosolic delivery of siRNA is reported. In this approach, siRNA is complexed with cationic arginine-functionalized gold nanoparticles by electrostatic interactions, with the resulting ensemble self-assembled onto the surface of fatty acid nanodroplets to form a NPSC/siRNA nanocomplex. The complex rapidly delivers siRNA into the cytosol through membrane fusion, a mechanism supported by cellular uptake studies. Using destabilized green fluorescent protein (deGFP) as a target, 90% knockdown was observed in HEK293 cells. Moreover, the delivery of siRNA targeting polo-like kinase 1 (siPLK1) efficiently silenced PLK1 expression in cancer cells with concomitant cytotoxicity.*

RNA interference (RNAi) is an endogenous pathway which silences gene expression at a post-translational level. The predominant strategy for RNAi uses small interfering RNA (siRNA) to target and cleave complementary mRNA, with concomitant inhibition of protein translation.[1] Since the discovery of RNAi by Fire et al.[2] and siRNA by Tuschl et al.,[3] the application of RNAi to knock down the expression of tumor-specific proteins or anti-apoptotic pathways has emerged as a novel therapeutic approach for cancer treatments.[4] siRNA is a double-strand RNA with a 21–23 base-pair length, and hence possesses a high molecular weight and multiple negative charges.[5] These physicochemical characteristics prevent passive diffusion across the membrane of most cell types for RNAi,[6] thus necessitating vectors for delivery of siRNA into the cytosol, where the incorporation of siRNA into RNAi machinery occurs.[7]

Recently, nanocarriers have been developed for siRNA delivery, including polymers,[8] liposomes,[9] and inorganic nanoparticles.[10] These siRNA vehicles generally enter cells through endocytic pathways, and are prone to entrapment within subcellular compartments.[11] This entrapment requires an increased dosage of siRNA, thus increasing the possibility of off-target effects.[12] Polyamine polymers and dendrimers can facilitate the escape of siRNA from endosomes[13] by taking advantage of the "proton sponge effect".[14] These highly cationic vehicles are, however, associated with cytotoxicity.[15] Therefore, delivery of siRNA into the cytosol remains a key challenge for the application of RNAi,[16] with direct cytosolic delivery providing the optimal outcome.

In this study, we demonstrate direct cytosolic delivery of siRNA using nanoparticle-stabilized nanocapsules (NPSCs). The stability of NPSCs relies on the supramolecular guanidine–carboxylate interactions between the arginine-functionalized gold nanoparticles (Arg-AuNPs) of the shell and the hydrophobic fatty acid "oil" components in the core (Figure 1a). This method produces nanocapsules capable of effective delivery of both small molecules[17] and proteins.[18] We hypothesized that electrostatic self-assembly of Arg-AuNPs and siRNA on the surface of the oil droplet would generate stable nanocapsules for siRNA delivery applications. We report herein the preparation of a NPSC/siRNA which provides cytosolic delivery of siRNA, as revealed through still and video microscopy of fluorescently labeled siRNA delivery. Moreover, we demonstrate that this cytosolic siRNA delivery process is mediated by direct fusion between

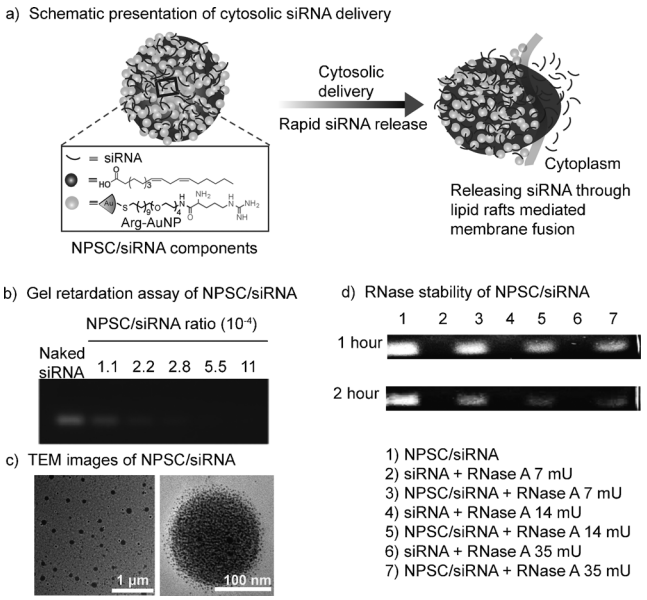

Figure 1. Preparation and characterization of NPSC/siRNA. a) NPSC/siRNA components and schematic presentation of NPSC-mediated cytosolic siRNA delivery. b) Gel electrophoresis study of NPSC/siRNA complexation at molar ratios ranging from 1.1×10^{-4} to 11×10^{-4}. c) TEM images of NPSC/siRNA. d) Protection of siRNA from RNase A digestion as evaluated by electrophoresis. 5 pmol of siRNA alone or complexed with NPSCs were incubated with 7, 14, and 35 mU RNase A at 37°C for indicated times.

[*] Y. Jiang, R. Tang, B. Duncan, Z. W. Jiang, Dr. B. Yan, R. Mout, Prof. Dr. V. M. Rotello
Department of Chemistry, University of Massachusetts Amherst
710 North Pleasant Street, Amherst, MA 01003 (USA)
E-mail: rotello@chem.umass.edu

[**] This work was supported by grants from the NIH (Grants EB014277 and GM077173).

Supporting information for this article is available on the WWW under http://dx.doi.org/10.1002/anie.201409161.

the NPSC/siRNA complex and the cell plasma membrane. The cytosolic delivery of siRNA resulted in highly efficient (90%) knockdown of a destabilized green fluorescence protein (deGFP) in deGFP-HEK293 cells. Moreover, the delivery of siRNA targeting polo-like kinase 1 (siPLK1) silenced PLK1 expression in cancer cells, thus resulting in pronounced toxicity. The effective siRNA gene silencing using NPSCs suggests the high potency of NPSC-facilitated direct cytosolic siRNA delivery as a platform to knock down targeted genes for disease treatment.

NPSCs were prepared according to our previous reports.[18] Briefly, a template emulsion was prepared by homogenizing Arg-AuNPs with linoleic acid in 5 mM phosphate buffer (pH 7.4). The template emulsion was transferred to an Arg-AuNP solution and incubated for additional 10 minutes to afford stabilized NPSCs. The NPSCs were then mixed with siRNA at different molar ratios and incubated at room temperature for 15 minutes, followed by a gel electrophoresis assay and Ribogreen assay to measure siRNA encapsulation. As shown in Figure 1b, with the NPSC to siRNA molar ratio increased from 1.1×10^{-4} to 11×10^{-4}, the migration of siRNA on the gel was gradually retarded. The binding at a molar ratio of 5.5×10^{-4} completely retarded siRNA from migration, with (91 ± 2)% of siRNA encapsulation, as determined by Ribogreen assay. This optimized NPSC to siRNA binding ratio was fixed for all subsequent intracellular delivery experiments. The encapsulation of siRNA had negligible effect on the morphology of the NPSCs, as revealed by transmission electron microscopy (TEM; Figure 1c). Dynamic light scattering (DLS) indicated the NPSCs and NPSC/siRNA formed nanoparticles with sizes of (149 ± 5) nm and (179 ± 8) nm, respectively, in diameter (see Table S1 in the Supporting Information). The slightly increased size of the NPSC/siRNA compared to that of a NPSC is consistent with swelling arising from the encapsulation of siRNA onto the NPSC surface. Additionally, the zeta potential of the NPSCs was made more negative from, −25.5 mV to −39.4 mV, for the NPSC/siRNA complex, thus confirming the successful encapsulation of siRNA by the NPSCs.

The encapsulation of siRNA by NPSCs efficiently protected siRNA against nuclease degradation, a prerequisite for the intracellular delivery of siRNA. As shown in Figure 1d, the treatment of free siRNA with ribonuclease A (RNase A; 7 mU) for 1 hour resulted in complete degradation of siRNA.[19] However, significant amounts of siRNA were still detected after the treatment of the NPSC/siRNA complex even at a much higher RNase A amount (35 mU) and a longer incubation (2 h). Similarly, the NPSC/siRNA complex efficiently protected siRNA against serum degradation (see Figure S1 in the Supporting Information). The enhanced enzymatic stability of siRNA with NPSC encapsulation may be ascribed to steric protection and neutralization of the siRNA charge, which together decreased the susceptibility of siRNA toward nuclease degradation.

We prepared a NPSC complex encapsulating fluorescently labeled siRNA (Cy3-siRNA) with a scrambled sequence to evaluate the delivery of siRNA.[20] The cellular uptake and subcellular localization of the NPSC/siRNA complex was then monitored using confocal laser scanning microscopy (CLSM). Significant intracellular accumulation of red fluorescence occurred when the cells were treated with the NPSC/Cy3-siRNA complex (Figure 2a). Significantly, the Cy3 fluorescence was evenly distributed within the whole cell, and had little overlap with the endosome/lysosome by using LysoTracker Green counterstaining. These CLSM studies suggest that the NPSC/siRNA complex was able to transport siRNA directly into the cytosol without the endosome/lysosome entrapment associated with polymer- or lipid-based siRNA delivery vehicles.[7] NPSC-mediated siRNA uptake is dependent on siRNA concentration. With the Cy3

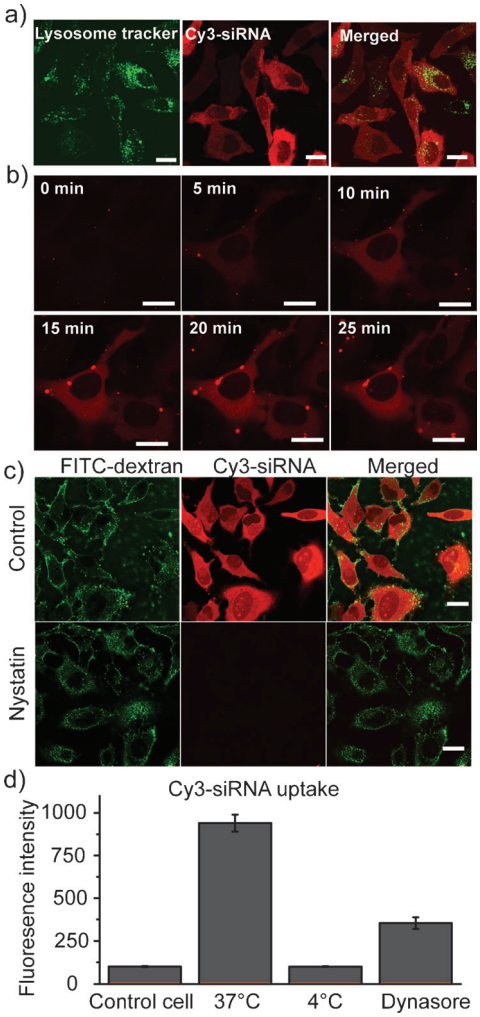

Figure 2. Cytosolic delivery of Cy3-labeled siRNA into HeLa cells. a) Confocal microscopy images of HeLa cells after a 1 hour treatment with 40 nM of the NPSC/Cy3-siRNA complex. siRNA are not colocalized with endolysosomes. Endosome/lysosome was stained with LysoTracker Green. Scale bars: 20 μm. b) Live cell imaging of rapid Cy3-siRNA release into the cytosol of HeLa cell by NPSCs. The 0 min label represents the starting point of release. Scale bars: 20 μm. c) FITC/dextran and NPSC/Cy3-siRNA were co-incubated with HeLa cells in the absence and presence of nystatin (100 $\mu g\,mL^{-1}$). d) Flow cytometry analysis of HeLa cells with NPSC/Cy3-siRNA treatment at 37°C, or at 4°C, or with a pre-treatment of dynasore (80 μM). The error bars represent the standard deviations of three parallel measurements.

siRNA increased from 12 nM to 36 nM, the Cy3 fluorescence intensity increased up to tenfold, and greater than 70% cells were Cy3 fluorescence positive, as measured by flow cytometry analysis (see Figure S2 in the Supporting Information).

The siRNA uptake and trafficking dynamics of NPSC siRNA delivery was investigated using time-lapse fluorescence imaging of Cy3-siRNA (Figure 2b and see Movie S1 in the Supporting Information). With the addition of the NPSC/Cy3-siRNA complex into HeLa cells, the fluorescence images of cells post-transfection were immediately captured at 1 minute intervals. Time-lapse imaging analysis revealed that cytosolic siRNA fluorescence could be recorded within 5 minutes of exposure of the NPSC/siRNA complex to cells, and the siRNA fluorescence was saturated after 20 minutes of incubation, thus demonstrating extraordinarily fast and efficient siRNA delivery using NPSCs. The siRNA fluorescence was evenly distributed within the whole-cell cytosol, further demonstrating that NPSC-mediated siRNA delivery enters cells and bypasses endo/lysosomes.[21]

In our previous study on protein delivery, we observed a similar even cytosolic distribution of GFP, thus prompting us to hypothesize that a membrane-fusion process was operative.[17] While there is circumstantial evidence of this mechanism, further studies were performed to test this hypothesis. The efficiency of membrane-fusion-mediated uptake is dependent on the cholesterol level in cell membrane.[22] To explore whether NPSCs delivered siRNA in a membrane-fusion pathway, HeLa cells were pretreated with nystatin (100 $\mu g\,mL^{-1}$), an inhibitor which has been used to deplete cholesterol from the plasma membrane,[23] prior to siRNA transfection. Meanwhile, FITC-labeled dextran, known to enter cells by endocytic pathways,[24] was co-incubated with cells to exclude the potential effect of nystatin treatment on endocytosis. Nystatin has no effect on the stability of the NPSC/siRNA complex, as revealed by the size of the NPSC/siRNA complex (determined by DLS) in the presence and absence of nystatin (see Figure S3 in the Supporting Information). The siRNA and FITC/dextran uptake was then monitored by CLSM imaging. As shown in Figure 2c, both dextran and NPSC/siRNA efficiently enter HeLa cells in the absence of nystatin, with low co-localization observed between dextran and siRNA, thus confirming non-endocytic uptake of the NPSC/siRNA complex. The treatment of nystain significantly blocked siRNA uptake, however, no uptake inhibition was observed for FITC/dextran. The siRNA uptake inhibition by nystatin treatment was further confirmed and quantified by flow cytometry analysis (see Figure S4 the Supporting Information). Nystatin pre-treatment significantly decreased the siRNA fluorescence intensity of HeLa cells, and the weak Cy3 fluorescence could be ascribed to the nonspecific binding of the NPSC/siRNA complex on cell surface, as confirmed by *z*-stack CLSM imaging of the NPSC/siRNA uptake (Figure S4). The above results indicated that nystain treatment did not block the endocytosis of FITC/dextran, but inhibited the membrane fusion of siRNA by depleting cell membrane cholesterol.

We further investigated the siRNA uptake efficiency by studying uptake at reduced temperature and by inhibiting dynamin. We pretreated HeLa cells at 4°C for 30 minutes before the exposure of NPSC/Cy3-siRNA, and the siRNA uptake was quantified by flow cytometry analysis and compared to that at 37°C. As shown in Figure 2d, Cy3 fluorescence arising from siRNA uptake was significantly decreased for cells with pretreatment at 4°C, similar to previous reports that the membrane-fusion process is a temperature-dependent process.[25] Meanwhile, the treatment of HeLa cells with dynasore (80 μM), an inhibitor of dynamin which regulates membrane fusion by expanding the fusion pores,[26] similarly reduced the cellular uptake of siRNA (Figure 2d). Taken together, the above cellular uptake studies indicate that NPSCs facilitated cytosolic siRNA delivery, which is a cholesterol-dependent membrane-fusion process.

We next evaluated the biocompatibility of the NPSC/siRNA delivery platform by treating destabilized GFP-expressing HEK293 cells with varied concentrations of NPSC/siRNA complexes, followed by a cell viability assay. With siRNA concentrations (complexed with NPSCs) from 10 nM to 60 nM the cells retained viabilities of greater than 80% (see Figure S5 in the Supporting Information), with the biocompatibility of NPSCs comparable to that of a commercial gene transfection reagent, Lipofectamine 2000 (see Figure S5 in the Supporting Information).

Having demonstrated the efficient yet safe cytosolic delivery of siRNA using NPSCs, we next investigated the efficacy of the NPSC-facilitated siRNA delivery to knock down targeted genes. As many disease-related proteins have short half-lives inside cells, an efficient siRNA delivery to silence a gene having a short half-life would have a high therapeutic index.[27] In this study, destabilized GFP (deGFP) with a half-life of around 2 hours was chosen as a testbed target gene. Stable-expressing deGFP-HEK293 cells were treated with a NPSC/siRNA complex targeting deGFP (NPSC/si_deGFP) or a scrambled siRNA (NPSC/siScr), and the deGFP expression profiles were monitored by CLSM imaging and flow cytometry analysis. As shown in Figure 4a, only very faint fluorescence signal was observed in the CLSM images when the cells were treated with the NPSC/si_deGFP complex, thus indicating the high efficiency of the NPSC-mediated deGFP knockdown. Flow cytometry analysis revealed that the NPSC/siRNA complex treatment (with 60 nM of si_deGFP) silenced the deGFP expression to a level below 10% of the blank control (Figure 3b and see Figure S6a in the Supporting Information). This gene silencing efficiency is substantially superior to the commercial lipid-based gene transfection reagents Lipofectamine 2000 (LPF2K; Figure 3b) and RNAi Max (see Figure S7 in the Supporting Information). The NPSC/si_deGFP complex silenced deGFP genes in a siRNA concentration dependent manner. With siRNA concentration increased from 20 nM to 60 nM the deGFP expression was gradually suppressed from 90% to 10% of the blank controls (see Figure S6b). As expected, no gene silencing was observed when the cells were treated with either naked si_deGFP or a NPSC/siRNA complex with a scrambled sequence (Figure 3b). As NPSCs delivered siRNA through a membrane-fusion pathway, we hypothesized that the pretreatment of HEK cells with nystatin to deplete cholesterol could block siRNA uptake and gene silencing. The GFP gene knockdown efficiency of

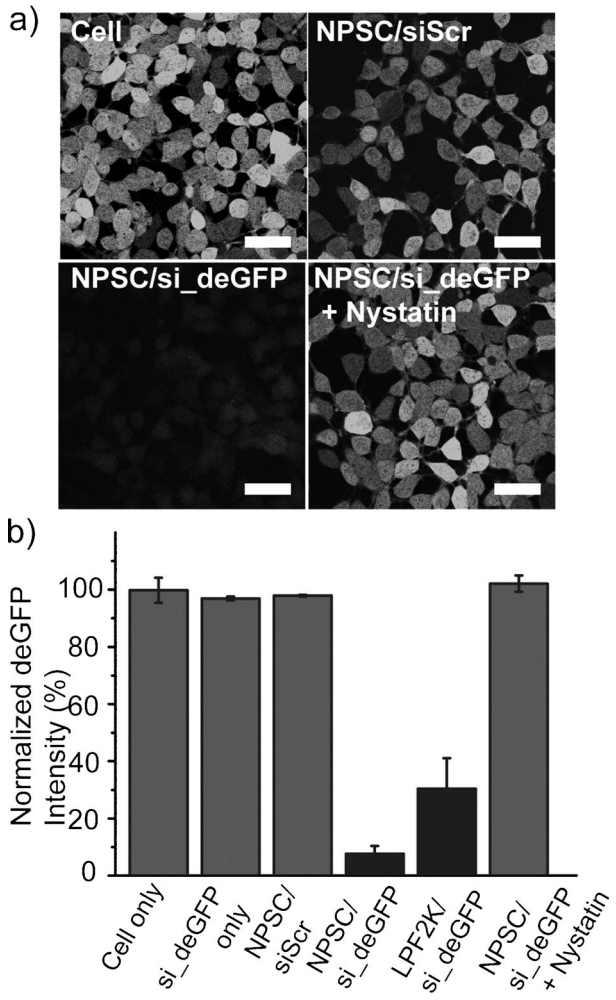

Figure 3. NPSC/siRNA delivery silenced the deGFP expression of deGFP-HEK293 cells. a) Confocal microscopy images of deGFP-HEK 293 cells without siRNA transfection (top left), with 60 nM of NPSC/siScr (top right), with 60 nM of NPSC/si_deGFP (bottom left), and with 60 nM of NPSC/si_deGFP with nystatin pretreatment (bottom right). Scale bars: 40 μm. b) Quantification of deGFP expression of deGFP-HEK 293 cells without treatment, with naked si_deGFP, NPSC/siScr, NPSC/si_deGFP, Lipofectamine 2000 (LPF2K)/si_deGFP, and NPSC/si_deGFP with nystatin pretreatment. 60 nM of si_deGFP or scrambled siRNA was used for transfection. The fluorescence intensity was measured by flow cytometry analysis and normalized to cells without treatment. The error bars represent the standard deviations of three parallel measurements.

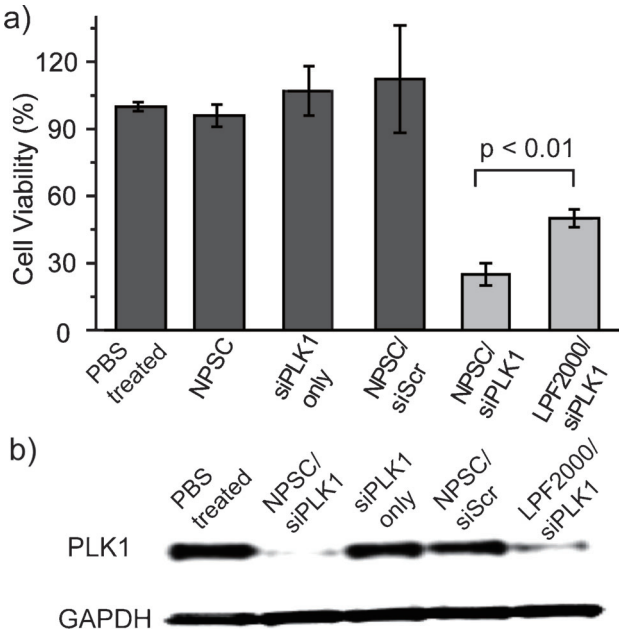

Figure 4. NPSC-mediated siPLK1 delivery in MDA-MB-231 cells. a) Cell viability of MDA-MB-231 cells treated with NPSC/siPLK1 or scrambled siRNA (40 nM). For the Lipofectamine 2000 control, 40 nM of siPLK1 was complexed with LPF2000 according to manufacturer's instructions. b) Representative PLK1 protein expression of MDA-MB-231 cells determined by Western blot analysis after incubation with 40 nM siPLK1 in NPSC/siPLK1 and controls. GAPDH expression was measured in all the samples to serve as an internal control.

HEK cells with nystatin or dynasore pretreatment, followed by NPSC/si_deGFP treatment, was significantly decreased, as indicated by the strong fluorescence in CLSM images (Figure 3a) and minor GFP gene knockdown in the flow cytometry analysis (Figure 3b and see Figure S8 in the Supporting Information). The GFP gene silencing results again confirmed that NPSC-facilitated delivery of siRNA is a cholesterol-dependent membrane fusion process, and the cytosolic siRNA delivery is superior to commercial reagents in terms of gene silencing efficiency.

Finally, we investigated the delivery of therapeutic siRNA. PLK1 was selected as a model therapeutic target. PLK1 is a key regulator of mitotic progression of cells, and is up-regulated in many types of cancer cells.[28] Inhibition of PLK1 activity or the depletion of PLK1 protein can induce mitotic arrest and prevent tumor cell proliferation.[29] Treatment of MDA-MB-231 cells with 40 nM NPSC/siPLK1 reduced cell viability to 30% whereas no change in viability was observed with naked or NPSC/siRNA scrambled controls (Figure 4a). Significantly, NPSC/siPLK1 inhibited cell proliferation with a higher efficiency than that of LPF2000. Knockdown of the intracellular PLK1 protein was determined by western-blot analysis. Essentially complete knockdown was observed when MDA-MB-231 cells were treated with NPSC/siPLK1 (40 nM siRNA; Figure 4b), and protein expression decreased by about 95% (see Figure S8 in the Supporting Information), a significantly greater knockdown than that of LPF2000/siPLK1 complexes.

In summary, we have demonstrated that NPSC/siRNA complexes provide a highly effective siRNA transfection strategy. Microscopy studies showed that these systems delivered siRNA directly to the cytosol, thus providing efficient utilization of the siRNA payload by avoiding endosomal sequestration. In addition, we proved that such a direct cytosolic siRNA delivery was a temperature-dependent membrane fusion process. Extremely efficient (>90% GFP gene silencing) and effective PLK1 silencing for cancer therapy was achieved with this vehicle, and was substantially better than commercial available systems. Taken together, NPSC/siRNA complexes provide effective tools for in vitro applications and promising platforms for biomedical delivery.

Experimental Section

See the Supporting Information for experimental details.

Received: September 16, 2014
Published online: November 12, 2014

Keywords: antitumor agents · cancer · gold · nanoparticles · RNA

[1] K. A. Whitehead, R. Langer, D. G. Anderson, *Nat. Rev. Drug Discovery* **2009**, *8*, 129 – 138.
[2] A. Fire, S. Xu, M. Montgomery, S. Kostas, S. Driver, C. C. Mello, *Nature* **1998**, *391*, 806 – 811.
[3] S. M. Elbashir, J. Harborth, W. Lendeckel, A. Yalcin, K. Weber, T. Tuschl, *Nature* **2001**, *411*, 494 – 498.
[4] a) C. V. Pecot, G. A. Calin, R. L. Coleman, G. Lopez-Berestein, A. K. Sood, *Nat. Rev. Cancer* **2011**, *11*, 59 – 67; b) M. E. Davis, J. E. Zuckerman, C. H. Choi, D. Seligson, A. Tolcher, C. A. Alabi, Y. Yen, J. D. Heidel, A. Ribas, *Nature* **2010**, *464*, 1067 – 1070.
[5] Y. Pei, T. Tuschl, *Nat. Methods* **2006**, *3*, 670 – 676.
[6] a) A. Schroeder, C. G. Levins, C. Cortez, R. Langer, D. G. Anderson, *J. Intern. Med.* **2010**, *267*, 9 – 21.
[7] a) Y. K. Oh, T. G. Park, *Adv. Drug Delivery Rev.* **2009**, *61*, 850 – 862; b) C. A. Alabi, K. T. Love, G. Sahay, H. Yin, K. M. Luly, R. Langer, D. G. Anderson, *Proc. Natl. Acad. Sci. USA* **2013**, *110*, 12881 – 12886; c) R. A. Petros, J. D. MeSimone, *Nat. Rev. Drug Discovery* **2010**, *9*, 615 – 627.
[8] a) D. J. Gary, N. Puri, Y. Y. Won, *J. Controlled Release* **2007**, *121*, 64 – 73; b) G. Grandinetti, T. M. Reineke, *Mol. Pharm.* **2012**, *9*, 2256 – 2267.
[9] S. C. Semple, A. Akinc, J. Chen, A. P. Sandhu, B. L. Mui, C. K. Cho, C. D. W. Y. Sah, D. Stebbing, E. J. Crosley, E. Yaworski, et al., *Nat. Biotechnol.* **2010**, *28*, 172 – 176.
[10] a) S. T. Kim, A. Chompoosor, Y. C. Yeh, S. S. Agasti, D. J. Solfiell, V. M. Rotello, *Small* **2012**, *8*, 3253 – 3256; b) D. Zheng, D. A. Giljohann, D. L. Chen, M. D. Massich, X. Q. Wang, H. Iordanov, C. A. Mirkin, A. S. Paller, *Proc. Natl. Acad. Sci. USA* **2012**, *109*, 11975 – 11980.
[11] a) G. Sahay, W. Querbes, C. Alabi, A. Eltoukhy, S. Sarkar, C. Zurenko, E. Karagiannis, K. Love, D. Chen, R. Zoncu, Y. Buganim, A. Schroeder, R. Langer, D. G. Anderson, *Nat. Biotechnol.* **2013**, *31*, 653 – 658; b) B. J. Hong, A. J. Chipre, S. T. Nguyen, *J. Am. Chem. Soc.* **2013**, *135*, 17655 – 17658.
[12] a) J. Kurreck, *Angew. Chem. Int. Ed.* **2009**, *48*, 1378 – 1398; *Angew. Chem.* **2009**, *121*, 1404 – 1426; b) S. Y. Duan, W. E. Yuan, F. Wu, T. Jin, *Angew. Chem. Int. Ed.* **2012**, *51*, 7938 – 7941; *Angew. Chem.* **2012**, *124*, 8062 – 8065.
[13] a) Y. J. Kwon, *Acc. Chem. Res.* **2012**, *45*, 1077 – 1088.
[14] a) N. D. Sonawane, F. C. Szoka, A. S. Verkman, *J. Biol. Chem.* **2003**, *278*, 44826 – 44831; b) M. V. Yezhelyev, L. Qi, R. M. O′Regan, S. Nie, X. Gao, *J. Am. Chem. Soc.* **2008**, *130*, 9006 – 9012; c) Y. Ding, Z. Jiang, K. Saha, C. S. Kim, S. T. Kim, R. F. Landis, V. M. Rotello, *Mol. Ther.* **2014**, *22*, 1075 – 1083.
[15] H. Lv, S. Zhang, B. Wang, S. Cui, J. Yan, *J. Controlled Release* **2006**, *114*, 100 – 109.
[16] a) J. K. Vasir, V. Labhasetwar, *Adv. Drug Delivery Rev.* **2007**, *59*, 718 – 728; b) S. H. Lee, S. H. Choi, S. H. Kim, T. G. Park, *J. Controlled Release* **2008**, *125*, 25 – 32; c) A. El-Sayed, S. Futaki, H. Harashima, *AAPS J.* **2009**, *11*, 13 – 22.
[17] X. C. Yang, B. Samanta, S. S. Agasti, Y. Jeong, Z. J. Zhu, S. Rana, O. R. Miranda, V. M. Rotello, *Angew. Chem. Int. Ed.* **2011**, *50*, 477 – 481; *Angew. Chem.* **2011**, *123*, 497 – 501.
[18] R. Tang, C. S. Kim, D. J. Solfiell, S. Rana, R. Mout, E. M. Velázquez-Delgado, A. Chompoosor, Y. Jeong, B. Yan, Z.-J. Zhu, C. Kim, A. Hardy, V. M. Rotello, *ACS Nano* **2013**, *7*, 6667 – 6673.
[19] a) V. Bitko, A. Musiyenko, O. Shulyayeva, S. Barik, *Nat. Med.* **2004**, *11*, 50 – 55; b) L. Han, J. Zhao, X. Zhang, W. Cao, X. Hu, G. Zou, X. Duan, X. J. Liang, *ACS Nano* **2012**, *6*, 7340 – 7351.
[20] a) B. Shah, P. T. Yin, S. Ghoshal, K. B. Lee, *Angew. Chem. Int. Ed.* **2013**, *52*, 6190 – 6195; *Angew. Chem.* **2013**, *125*, 6310 – 6315; b) H. Lu, D. Wang, S. Kazane, T. Javahishvili, F. Tian, F. Song, A. Sellers, B. Barnett, P. G. Schultz, *J. Am. Chem. Soc.* **2013**, *135*, 13885 – 13891.
[21] Z. H. Zhang, W. G. Cao, H. L. Jin, J. F. Lovell, M. Yang, L. L. Ding, J. Chen, I. Corbin, Q. M. Luo, G. Zheng, *Angew. Chem. Int. Ed.* **2009**, *48*, 9171 – 9175; *Angew. Chem.* **2009**, *121*, 9335 – 9339.
[22] a) M. Yang, H. L. Jin, J. Chen, L. L. Ding, K. K. Ng, Q. Y. Lin, J. F. Lovell, Z. H. Zhang, G. Zhang, *Small* **2011**, *7*, 568 – 573; b) Q. Y. Lin, J. Chen, K. K. Ng, W. G. Cao, Z. H. Zhang, G. Zheng, *Pharm. Res.* **2014**, *31*, 1438 – 1449; c) K. C. Partlow, G. M. Lanza, S. A. Wickline, *Biomaterials* **2008**, *29*, 3367 – 3375.
[23] J. J. Lu, R. Langer, J. Chen, *Mol. Pharm.* **2009**, *6*, 763 – 771.
[24] K. T. Love, K. P. Mahon, C. G. Leyins, K. A. Whitehead, W. Querbes, J. R. Dorkin, J. Qin, W. Cantley, L. L. Qin, T. Racie, M. Frank-Kamenetsky, K. N. Yip, R. Alyarez, D. W. Y. Sah, A. Fougerolles, K. Fitzgerald, V. Koteliansky, A. Akinc, R. Langer, D. G. Anderson, *Proc. Natl. Acad. Sci. USA* **2010**, *107*, 1864 – 1869.
[25] a) S. Martens, H. T. McMahon, *Nat. Rev. Mol. Cell Biol.* **2008**, *9*, 543 – 556; b) A. Grafmüller, J. Shillcock, R. Lipowsky, *Phys. Rev. Lett.* **2007**, *98*, 218101 – 218104; c) S. M. Roy, M. Sarkar, *J. Lipids.* **2011**, 528784.
[26] Y. Sun, P, Tien, *Crit. Rev. Microbiol.* **2013**, *39*, 166 – 179.
[27] M. D. Krebs, O. Jeon, E. Alsberg, *J. Am. Chem. Soc.* **2009**, *131*, 9204 – 9206.
[28] a) Y. Degenhardt, T. Lampkin, K. Strebhardt, A. Ullrich, *Nat. Rev. Cancer* **2006**, *6*, 321 – 330; b) J. O. McNamara, E. R. Andrechek, Y. Wang, K. D. Viles, R. E. Rempel, E. Gilboa, B. A. Sullenger, P. H. Giangrande, *Nat. Biotechnol.* **2006**, *24*, 1005 – 1015.
[29] Y. D. Yao, T. M. Sun, S. Y. Huang, S. Dou, L. Lin, J. N. Chen, J. B. Ruan, C. Q. Mao, F. Y. Yu, M. S. Z, J. Y. Zang, Q. Liu, F. X. Su, P. Zhang, J. Lieberman, J. Wang, E. W. Song, *Sci. Transl. Med.* **2012**, *4*, 130ra48.